HHS Public Access

Author manuscript

Ann Biomed Eng. Author manuscript; available in PMC 2016 June 01.

Published in final edited form as:

Ann Biomed Eng. 2015 June ; 43(6): 1348–1362. doi:10.1007/s10439-014-1094-5.

COMPUTATIONAL MITRAL VALVE EVALUATION AND POTENTIAL CLINICAL APPLICATIONS

Krishnan B. Chandran[1] and **Hyunggun Kim**[1,2,#]

[1]Department of Biomedical Engineering, The University of Iowa, Iowa City, Iowa 52242, USA

[2]Division of Cardiovascular Medicine, Department of Internal Medicine, The University of Texas Health Science Center at Houston, Houston, Texas 77030, USA

Abstract

The mitral valve (MV) apparatus consists of the two asymmetric leaflets, the saddle-shaped annulus, the chordae tendineae, and the papillary muscles. MV function over the cardiac cycle involves complex interaction between the MV apparatus components for efficient blood circulation. Common diseases of the MV include valvular stenosis, regurgitation, and prolapse. MV repair is the most popular and most reliable surgical treatment for early MV pathology. One of the unsolved problems in MV repair is to predict the optimal repair strategy for each patient. Although experimental studies have provided valuable information to improve repair techniques, computational simulations are increasingly playing an important role in understanding the complex MV dynamics, particularly with the availability of patient-specific real-time imaging modalities. This work presents a review of computational simulation studies of MV function employing finite element (FE) structural analysis and fluid-structure interaction (FSI) approach reported in the literature to date. More recent studies towards potential applications of computational simulation approaches in the assessment of valvular repair techniques and potential pre-surgical planning of repair strategies are also discussed. It is anticipated that further advancements in computational techniques combined with the next generations of clinical imaging modalities will enable physiologically more realistic simulations. Such advancement in imaging and computation will allow for patient-specific, disease-specific, and case-specific MV evaluation and virtual prediction of MV repair.

Anatomy, function and diseases of the mitral valve

Heart valves play a very important role in maintaining unidirectional flow in the circulation by opening and closing efficiently at appropriate times during the cardiac cycle. The aortic and mitral valves in the left heart are subjected to high pressures and the leaflets undergo complex motion and deformation associated with high in-plane and bending stresses. The mitral valve (MV) between the left atrium and the left ventricle enables efficient filling of the left ventricle during diastole and closes rapidly at the beginning of the ventricular contraction preventing regurgitation of blood back into the left atrium during the isovolumic

[#]Correspondence: Hyunggun Kim, Ph.D. Division of Cardiovascular Medicine Department of Internal Medicine The University of Texas Health Science Center at Houston 6431 Fannin St, MSB 1.246 Houston, Texas 77030, USA Phone: +1-713-486-2342 Fax: +1-713-500-6556 Hyunggun.Kim@uth.tmc.edu.

contraction phase. The MV apparatus consists of the two asymmetric leaflets (cusps), the three-dimensional (3D) saddle-shaped annulus, the chordae tendineae, and the papillary muscles.[41] A schematic of the MV apparatus is shown in Figure 1. The base of the anterior and posterior leaflets form the mitral annulus that is attached to the left ventricular and aortic walls and the aortic root.[17,50] The mitral annulus, consisting of dense collagenous tissue surrounded by muscle fibers, undergoes complex 3D motion during the cardiac cycle.[43,88] The tissue of the MV leaflets consists of collagen-reinforced endothelium, striated cardiac muscle cells, smooth muscle cells, and nonmyelinated nerve fibers.[66,84] Morphologic evidence of extensive innervation in the human heart and valve leaflets have been reported although the role and mechanisms of these nerves in independent MV movement is still uncertain.[66] The leaflets are essentially one continuous piece of tissue with indentations along the free edges. Two regularly spaced indentations, called commissures, separate the tissue into the anterior and posterior leaflets. The slightly larger anterior leaflet is approximately semilunar in shape compared to the quadrangular-shaped posterior leaflet.[17,59] The combined surface area of the leaflets is approximately twice the area of the mitral orifice. Such a configuration results in a large area of coaptation of the two leaflets when the valve closes. Along the free edge of the leaflets, the chordae tendineae are inserted through multiple locations. The other end of the chordae are attached to the tips of the anterolateral and posteromedial papillary muscles. The chordae are classified as the thinner marginal chordae inserting into the free edge of the leaflets and the thicker basal chordae inserting more towards the annulus. These areas of the leaflets where the chordae are inserted is the rough zone with thicker tissue compared to the rest of the leaflets (i.e., the clear zone) where thinner and translucent tissue is found.

MV function during the opening and closing phases is a result of complex interaction of the leaflets, the annulus, the chordae and the papillary muscles.[17,47] At the beginning of diastole, as the ventricle relaxes and the ventricular pressure falls below that of the atrium, the MV opens into a funnel shape for rapid ventricular filling. Ventricular wall motion and papillary muscle contraction during this phase also aids in the separation of the leaflets for efficient ventricular filling.[7] Ventricular filling results in the formation of two large vortices behind each leaflet and the shear forces from the vortices move the leaflets towards closure prior to ventricular contraction. Atrial contraction at that time once again forces the leaflets towards fully open position with additional filling of blood in the ventricle.[75] Ventricular contraction at the beginning of systole and rapid rise in pressure in the chamber force the leaflets to close. The two leaflets contact each other at the respective rough zone and are stabilized by the chordae while sustaining the remaining leaflet surfaces in a flat or slightly billowing shape into the left atrium due to the high transvalvular pressure.[84] In the normal function of a healthy MV, the valve opening is initiated with the pressure difference between the atrium and the ventricle of the order of 1 mmHg and the leaflets close efficiently allowing minimal backflow or regurgitation of blood into the left atrium during the closing phase.

Common diseases of the MV include valvular stenosis, regurgitation, and prolapse.[97] Mitral stenosis is usually caused by rheumatic heart diseases resulting in progressive leaflet thickening, scarring, and calcification. Stenosis leads to narrowing of the valve orifice in the fully open position with significant increase in pressure drop across the valve. Elevated

pulmonary venous and left atrial pressures may lead to atrial enlargement, fibrillation, and thromboembolism.

Mitral regurgitation (MR) is the leakage of blood from the ventricle to the atrium during systole. MR is the result of structural or functional abnormalities of the MV apparatus, and the prevalence of MR is 1.7% adjusted to the entire US population.[39] Common structural causes of MR include annular dilatation, chordal rupture and elongation, and papillary muscle anomalies. Functional abnormalities causing MR include myxomatous MV diseases, leaflet prolapse, rheumatic heart diseases, infective endocarditis, coronary artery diseases and cardiomyopathy. Acute severe MR results in increase of left atrial and pulmonary venous pressures with pulmonary congestion and edema. Chronic MR in advanced stages results in contractile dysfunction, ventricular remodeling and heart failure.[30]

MV prolapse is the excessive billowing of one or both leaflets into the left atrium during systole. Many patients with normal MV leaflets have MV prolapse with little or no MR and are asymptomatic. If a patient has myxomatous valvular diseases, MV prolapse with moderate MR may be under high risk of cardiovascular complications requiring interventional treatment.

MV repair techniques

MV repair (MVR) is the most popular and most reliable surgical treatment for early MV pathology.[2,37] MVR was limited to a small percentage of MV treatment in the early days, but now cardiothoracic surgeons perform MVR in more than 90% of interventional cases.[26,40] In the early days, a plication technique in the commissural region was commonly utilized for severe MR.[48] Ring annuloplasty techniques were introduced to repair annular dilation and improve leaflet coaptation.[13] Recent surgical advancements including leaflet resection, chordal replacement, and chordal shortening/transposition in addition to more sophisticated annuloplasty rings have resulted in a markedly increased repair rate.[60,61]

Degenerative MV diseases are commonly involved with annular dilation. Ring annuloplasty focuses on restoring a normal size and shape of the mitral annulus. A number of studies have revealed the efficiency of ring annuloplasty in providing improved durability of MVR compared to ringless repairs.[23,67] There are a large variety of rings available with different shapes, sizes, and materials (2D vs. 3D, complete vs. partial, rigid vs. flexible, etc.).[11,31] Some are implanted regardless of case type and others are disease-specifically designed. Although ring annuloplasty is employed in almost every MVR, the approach to patient-specific ring sizing and selection often appears arbitrary and inconsistent.[12] Long-term clinical results of many of these rings are still under investigation.[20,85]

Quadrangular resection of redundant posterior leaflet segment is one of the standard repair techniques.[15,16] Clinical long-term outcomes demonstrate triangular and quadrangular resections as reliable and reproducible surgical repair techniques for treatment of prolapsed MV leaflets.[13,80] Several pitfalls of leaflet resection techniques include decreased leaflet coaptation due to forced remodeling of the valvular structure, and a remaining risk of systolic anterior motion (SAM) with obstruction of left ventricular outflow tract.[38,62] Sliding

leaflet techniques combined with upsizing ring annuloplasty are effective to reduce the incidence of SAM.[35]

Ruptured chordae commonly leads to severe MR and acute malfunction of the MV as the chordae play a critical role in preventing the leaflets from prolapsing. Resection is a common technique to repair ruptured chordae. Another interventional treatment for ruptured chordae is chordal replacement using artificial chordae.[10,15] Chordal replacement can be performed either with or without ring annuloplasty.[34] Expanded polytetrafluoroethylene (ePTFE) sutures are popular as neochordae for chordal replacement, and clinical studies of its long-term effect revealed safe, effective, and reproducible repair outcomes.[10,27] The primary difficulty in using artificial chordae is to determine the suture length.[15] Artificial chordae can degenerate, calcify, and rupture due to imbalanced material characteristics between native and artificial chordae.[14]

Edge-to-edge repair (ETER) technique restores leaflet coaptation by anchoring the prolapsing segment to the opposing leaflet with the use of sutures or clips.[4,32] ETER provides reduced complications and low morbidity/mortality, particularly benefiting high risk patients for thoracotomic surgery.[87] Clinical studies demonstrated the safety and effectiveness of percutaneous ETER in comparison with standard MVR.[4,32] Multiple attempts are often required to place a clip, sometimes two clips are placed in ~30% of the procedures, and ~10% of the procedures are aborted due to complications.[32] There are several concerns in ETER techniques. ETER without ring annuloplasty may lead to recurrent MR and a high risk of reoperation.[8,36] ETER can also restrict the mitral orifice resulting in mitral stenosis.[31] For treatment of MR reoccurrence following ETER, MV replacement may be required rather than repair.[5]

One of the unsolved problems in MVR is to predict the optimal repair strategy for each patient. Much of the problem lies in the difficulty in fully understanding the MV pathophysiology which predisposes it to dysfunction and insufficiency. The majority of cases have complex involvement of multiple pathologies including annular dilation, leaflet thickening, excessive/restricted leaflet motion, chordal elongation/rupture, papillary muscle elongation/rupture, calcification of the MV structures, etc. A thorough understanding of MV dynamics and structural characteristics of the MV apparatus is imperative for accurate diagnosis and focused treatment of MV pathology.

Computational simulations for functional evaluation and treatment planning

With the advent of high-speed computational hardware and software and significant advances in computational mechanics (both in solid and fluid), computational simulations are increasingly playing an important role in understanding normal anatomy and physiology, functional alterations in pathophysiology, development and progression of diseases, interventional and surgical planning, and design of implants.[1,17,18] In the cardiovascular system, typical examples of the application of computational simulations include flow dynamics analysis in the etiology and development of atherosclerotic plaques, prediction of rupture of aneurysms, and surgical planning for Fontan procedure, structural and

hemodynamic analysis in the understanding of native heart valve function and etiology of valvular diseases, and design and analysis of implants such as heart valves, vascular grafts, and stents. Computational simulations in the cardiovascular system have routinely employed finite element (FE) structural analysis of biological soft tissue such as the arterial wall and valve leaflets, and computational fluid dynamics (CFD) in complex geometries such as curved and bifurcated arterial segments. More recently a unified fluid-structure interaction (FSI) analysis for realistic simulation of the complex interaction between the soft tissue with the flowing blood in the circulatory system are being systematically employed. Morphologically realistic 3D geometry of the organs of interest are available from the state-of-the-art imaging modalities including ultrasound, cine-computed tomography, and magnetic resonance imaging. Patient-specific geometric information is now being increasingly employed in computational simulations.

In the case of native human heart valves, FE analysis have been utilized for the past five decades in order to understand the relationship between stress concentration and etiology of leaflet calcification. CFD analysis have been employed to compare alterations in flow dynamics with the onset of diseases such as valvular regurgitation and congenital valve malformations. More recently, FSI analysis has been attempted to understand the complex dynamics of aortic and mitral valvular function.

In the following sections, we review the current status of computational simulations for our increased understanding of MV dynamics. We also present more recent simulation outcomes towards potential applications of computational simulation approaches in the assessment of MVR techniques and pre-surgical planning of repair strategies.

Previous computational studies and current status of computational approaches

Abnormalities in morphologic deformation, stress distribution in the leaflets and chordae, and leaflet coaptation play an important role in modulating MV function. Computational simulation of MV function provides complex biomechanical information pertaining to pathophysiologic alterations. Computational evaluation of these abnormal pathologic features of the complex MV apparatus in each patient can provide improved diagnosis and better prediction of outcomes following MVR.

Dynamic computational simulations of the MV apparatus are very valuable in our understanding of the complex interaction among the various valvular components, the relationship between mechanical stresses and valve failure, and the effectiveness of MVR towards restoring normal MV function. Kunzelman and colleagues reported a series of FE studies of the MV.[54,56-58] The first 3D MV model was reconstructed from an excised porcine valve incorporating collagen fiber orientation and nonlinear anisotropic material properties of the leaflets and regional tissue thickness variations.[54] The effect of annular contraction and dilatation on leaflet coaptation and stresses was assessed. This group also performed FE evaluation of ring annuloplasty for treatment of annular dilatation.[58] Salgo et al. investigated the effect of the saddle shaped annulus on stress distributions across the MV leaflets.[81] Performing computational analysis with a flat annulus and comparing the results

with increasing saddle heights, their study demonstrated the effect of the saddle shape in reducing the peak stresses. Lim et al. developed a computational MV model introducing the asymmetric anterior and posterior leaflet geometry obtained from sonomicrometry data in a sheep model.[63] They demonstrated the heterogeneity of stress distribution during peak pressure loading and nonhomogeneous leaflet stretching during the isovolumic relaxation phase. Maisano et al. performed a computational study to assess the effect of annuloplasty ring shape in treatment of functional MR under extreme leaflet tethering.[64] Their study demonstrated that a dog bone-shaped ring was more effective compared to a conventional D-shaped ring in minimizing regurgitation. This study and that of Votta et al.[94] suggested a disease-specific annuloplasty prosthesis strategy for improved repair outcomes. Prot et al. reported a modeling study to assess the effect of annular shape as well as the role of the anterior secondary chordae on displacement of the leaflets.[71] Computational studies have also been effectively used[6,25,95] in assessing the efficacy of ETER[4] for MR treatment.

Most of these models above utilized MV geometries obtained either by parametric modeling, by image reconstruction of markers placed on the valvular apparatus or from excised valve specimens. More recently, MV modeling strategies have been transitioning to morphologically realistic patient-specific MV modeling utilizing real-time 3D imaging data.[70,92,93] The majority of the earlier computational models employed linear elastic material behavior of the valve structures. Recent modeling approaches have attempted to employ more realistic nonlinear hyperelastic anisotropic material properties for the MV apparatus components.

Our group developed a novel computational MV evaluation strategy by combining 3D echocardiography and FE simulation techniques, and demonstrated four representative clinical cases (normal, mild MR, severe MR, and ruptured chordae) of patient-specific MV evaluation (Figure 2).[76] The normal MV revealed complete leaflet coaptation with no MR. The MV with a relatively small degree of annular dilation accompanied by mild MR showed increased stresses across the leaflets and reduced leaflet contact pressure distribution. The degenerative MV with large annular dilation accompanied by severe MR demonstrated markedly asymmetric high stress distribution widely spreading along the radial direction and a large lack of leaflet contact indicating incomplete leaflet closure. The MV with ruptured posterior chordae displayed extremely asymmetric and large stresses as well as flail posterior leaflet prolapse with no leaflet coaptation in the regurgitant region. These patient-specific and case-specific computational MV evaluation studies corresponded well to the standard clinical echocardiographic MV evaluation data, and provided additional quantitative information pertaining to normal and pathologic MV function from a biomechanical perspective. We have found that a patient MV with large annular dilation can experience abnormal distribution of large stresses even when echocardiographic data show a relatively sufficient leaflet coaptation with no significant MR. A chronic condition under such large stresses within the leaflet and chordal structure may lead to MR development. Patient-specific biomechanical evaluation of MV function using clinical imaging modalities and computational analysis techniques can help us better understand pathophysiologic MV characteristics and predict potential MR development.

Computational structural simulations commonly specify uniform blood pressure loading on the leaflet surfaces to determine leaflet deformations and stress distributions during valve dynamics. Such simulations ignore the non-uniform pressure and shear stress loading on the leaflets induced by local blood flow dynamics and cannot provide information of fluid mechanical alteration across the MV following the onset of diseases or MVR with considerable morphologic changes of the MV apparatus. In-vitro fluid mechanical studies of MV dynamics demonstrated a flow jet into the left ventricle during the ventricular filling phase, formation of two large counter-rotating vortices, and shear stress effect on leaflet motion during the closing phase.[72,75] An in-vitro study has been also reported to investigate the alterations of fluid dynamics in the ventricular chamber following ETER.[83] Long-term effects of such alterations in the local fluid mechanics may be evaluated by employing FSI analysis. In the case of heart valve dynamics, such an analysis is extremely challenging due to large and complex deformation of the leaflets during the cardiac cycle.[90] De Hart et al.[28] performed 3D FSI simulations for the aortic valve, and Kunzelman et al.[55] reported a FSI analysis for MV dynamics. However, these studies included non-physiologic assumptions in the simulations such as much stiffer material properties of the leaflets than native valve tissue and non-physiologic flow Reynolds numbers to overcome numerical difficulties.

Efforts have been focused on the creation of morphologically realistic patient-specific geometry of the MV apparatus, the use of realistic soft tissue material properties of the valvular structures, and the development of improved FSI algorithms to overcome the computational restrictions listed above. These developments will further enhance the capability of computational evaluation approaches to better understand normal MV dynamics and functional alterations with valvular pathologies, helping to improve patient-specific pre-surgical planning of repair techniques towards best restoring normal MV function.

3D echocardiography for patient-specific MV imaging

Echocardiography is the standard noninvasive clinical imaging modality to examine cardiac function and valvular diseases. Echocardiography not only offers patients a cost effective valve examination but also provides physicians both morphologic and functional information of the MV. Echocardiography can accurately capture detailed morphologic alterations of the fast moving MV structure over the cardiac cycle. Color Doppler ultrasound allows us to identify the direction and velocity of blood flow around the MV. Primary weaknesses of echocardiography include low resolution for chordae imaging, a restricted window view in some patients, low signal-to-noise ratio, acoustic reflection, ultrasound attenuation, and relatively high inter-observer variability. In particular, the comprehensive chordae structure is hard to be identified in echocardiographic imaging while the location of the papillary muscles attached to the left ventricle is clearly detected.

Other noninvasive 3D cardiac imaging modalities include computed tomography (CT) and magnetic resonance imaging (MRI). Cardiac CT and MRI can provide relatively clearer images with a high signal-to-noise ratio and comprehensive cross-sectional images of the patient's heart compared to echocardiography. Primary disadvantages of cardiac CT and MRI in MV imaging are the difficulty in capturing the moving valve leaflets and high cost.

Due to these limitations, cardiac CT and MRI have been less popular for assessment of MV function than echocardiography. However, cardiac CT and MRI may play an important role to provide detailed morphologic and functional information of the MV in addition to echocardiography in the near future with advancement of imaging technologies.

Recent technical advances in echocardiography offer an effective 3D imaging of the MV and help physicians improve diagnosis of MV diseases. Current 3D echocardiography systems utilize thousands of imaging elements in the matrix array and provide excellent 3D images of the MV in real time.[24,42] Although 2D echocardiography is still the standard imaging modality for heat valve evaluation, 3D assessment benefits MV evaluation due to the complex MV structure. In particular, real time 3D echocardiography provides an excellent tool to characterize mitral annular shape,[33,46] diagnose MV prolapse and leaflet perforation,[3,82] and measure MV area, [9,99,101] and is now widely being used for diagnosis of MV pathology and pre-surgical planning prior to MVR.

Image processing and graphic rendering techniques can be utilized to create and characterize 3D MV geometry in vivo using 3D echocardiography.[21,69,79] Our group and others have developed algorithms to extract MV geometry from 3D transesophageal echocardiographic (TEE) data, create a patient-specific computational MV model, and perform FE simulations of MV function.[65,76,78,89,92]

In a standard 3D TEE protocol, a patient is placed in the left lateral decubitus position such that maximal flexion of the neck with chin-to-chest can be obtained. A TEE probe is inserted with guidance offered by the operator's left index finger following bite block insertion, and placed at the esophagolaryngeal junction. The probe is advanced to approximately 40 cm from the incisors, and imaging is performed with wide angle acquisition mode. The 3D MV structure is imaged at the transgastric and mid-esophageal locations. In addition to 3D MV imaging, pulsed wave and continuous wave measurements across the MV are acquired, and color Doppler can be utilized to capture 3D MR.

Computational 3D MV modeling protocols are often composed of multiple sub-algorithms including ECG-gated 3D TEE image data acquisition, MV leaflets and apparatus segmentation, image registration, 3D reconstruction, mesh creation, chordae tendineae creation, and incorporation of 3D dynamic motion of the mitral annulus and papillary muscles.

Patient-specific 3D MV modeling and analysis

Early computational studies of MV dynamics utilized simplified parametric FE models to simulate MV function. Recently several research groups reported patient-specific MV modeling strategies for FE evaluation of MV dynamics. Votta et al. performed 3D reconstruction of patient-specific annular geometry utilizing 3D echocardiographic data.[92] Jassar et al. developed a 3D MV modeling technique to quantitatively assess the MV structure from 3D TEE data, and demonstrated excellent reproducibility of 3D MV modeling.[44] This group also performed in-vivo MV modeling and stress analysis using their semi-automated 3D image processing and modeling system incorporated.[69,100] Mansi et al. presented an integrated framework for volumetric FE modeling of the MV apparatus,

performed a sensitivity analysis, and evaluated MV function in 25 patients.[65] Our group developed a novel algorithm for MV modeling including segmentation of the MV apparatus geometry and patient-specific annular motion over the cardiac cycle.[78] We found that the incorporation of dynamic annular motion clearly reduced regions with large stresses and helped to determine improper leaflet coaptation. We also presented case reports of normal MV, mild MR, severe MR, and ruptured chordae using this novel computational MV evaluation strategy.[76]

Other imaging modalities can be also used for computational MV modeling. Stevanella et al. created a patient MV model utilizing cardiac MRI data containing time-dependent papillary muscle location information.[86] Kaji et al. studied the geometric dimensions of the mitral annulus and papillary muscles using clinical 3D MRI.[45] Wang and Sun presented a normal patient MV model reconstructed from cardiac CT data including information of leaflet thickness, chordal structure and distribution, papillary muscle location, and annular motion.[96]

Although these studies reported excellent advancement in computational MV modeling and analysis, there are several general limitations and simplifications that need to be resolved and improved. Actual material property information of patient MV tissue is not available. Experimentally determined material property data of porcine MV tissue or excised human tissue from MVR or cadaver are generally utilized. Another primary assumption is related to modeling of the chordae tendineae. As current imaging modalities cannot provide a complete description of structure and distribution of the chordae in vivo, general anatomic information from clinical studies is commonly implemented into computational MV modeling for the chordae.[78,92] Accurate computational modeling to fully understand the role of the chordae on coaptation and billowing of the leaflets will only be available with advancements in imaging modalities to provide anatomic details of the chordae length and distribution. Lastly, incorporation of realistic fluid-induced effects on the MV structure is required to more realistically simulate patient-specific MV function. It is expected that more advanced patient-specific FSI strategies that can simulate MV dynamics under the physiologic conditions will resolve this limitation.

Computational simulation for prediction of MV repair

Early studies by Kunzelman et al. demonstrated FE simulations using a parametrically created MV model to assess improved leaflet coaptation and reduced leaflet/chordal stresses following ePTFE suture replacement for ruptured chordae.[53] They also determined the effect of varying number, size, and length of ePTFE sutures.[73,74] Recently, our group demonstrated a novel evaluation protocol to create a virtual MV model using 3D TEE data in a patient with posterior chordal rupture, and determined the effect of chordal replacement on restoring MV function following virtual chordal replacement (Figure 3).[77] We found that extremely large stresses occurred in the neighboring intact posterior leaflet tissue and chordae of the MV with ruptured chordae, and these large stresses were markedly reduced when virtual chordal replacement was performed. Similar computational strategies can provide quantitative information pertaining to biomechanical and physiologic characteristics

of pathologic MVs with ruptured chordae and predict functional improvement following virtual chordal replacement using ePTFE sutures.

Several groups have demonstrated FE simulation studies for ring annuloplasty. Kunzelman et al. compared flexible and rigid annuloplasty rings using their parametric MV model, and demonstrated that both rings improved coaptation while the flexible ring further reduced leaflet and chordal stresses than the rigid ring.[58] Maisano et al. utilized the same parametric MV model and demonstrated that dog bone-shaped ring prosthesis provided better performance in the correction of functional MR than standard D-shaped rings.[64] Votta et al. reported a comparative simulation study between the Physio and the Geoform annuloplasty rings.[94] Wong et al. demonstrated the effect of the Physio II and the IMR ETlogix rings.[98] These studies employed a parametric MV model, partial patient-specific MV geometry or animal MV model. Stevanella et al. created a patient MV using CMR data and performed FE simulations of ring annuloplasty.[86] Our group recently employed a 3D TEE-based patient-specific MV model which revealed severe MR, incorporated patient-specific annular motion data, and demonstrated a virtual ring annuloplasty simulation successfully restoring leaflet coaptation (Figure 4).[22]

Votta et al. performed FE simulations of ETER intervention and demonstrated that diastolic peak stresses in the leaflets were comparable with those found during systole.[95] Others investigated the effects of size and location of stitching during ETER via computational approaches.[6,25] Mansi et al. developed an integrated framework for ETER simulation and reported FE-predicted repair outcomes using 25 patient data.[65]

Although these FE studies demonstrated excellent cases of computational evaluation and prediction of different types of MVR, there are some limitations and simplifications that need to be further investigated and improved. The primary limitation of computational prediction of MVR is the limited availability of the actual material properties of patient MV tissue. This issue is involved in any patient-specific computational simulation studies of MV function. Another limitation in MV modeling is that acquisition of actual geometric information of the entire patient chordae structure is not feasible utilizing current imaging techniques. It is expected that advancement of imaging technologies will help to resolve these issues.

If patient-specific virtual evaluation of MVR can be conducted prior to actual surgery, i.e., prospectively, this computational prediction is a promising strategy to help pre-surgical planning of MVR. Rigorous validation studies to compare with clinical post-MVR outcomes are still required to utilize these virtual MVR simulation techniques for clinical application. Moreover, computational prediction of MVR should be carefully interpreted as the long-term effect of the MVR cannot be provided by this approach. A longitudinal post-MVR evaluation study is required to fully understand the relationship between computational prediction of MVR and the long-term effect following the MVR.

Fluid-structure interaction analysis

The FE analyses described above can be successfully employed to study deformation and stress distribution of the MV leaflet and chordal structures. FE evaluation of MV function

allows us to assess abnormal alterations of morphologic and physiologic characteristics of the MV following the onset of diseases or the efficacy of various MVR techniques. However, the general loading conditions in FE simulations of MV function adopt simplified and uniformly distributed blood pressure magnitudes on the leaflet surface structures during the cardiac cycle. Such loading ignores the effect of variations in pressure and shear stresses on the valvular structures induced by complex flow dynamics around the MV apparatus. Furthermore, long-term effects of alterations in flow dynamics such as those anticipated with ETER cannot be assessed. In order to incorporate these effects in computational simulation, FSI analysis is necessary. As pointed out earlier, limited applications of FSI analysis for heart valve dynamics have been reported in the literature and even these studies were not thoroughly exercised for physiologically realistic flow regimes in aortic or mitral valve dynamics. De Hart et al. reported a FSI study for the aortic valve.[28] However, the material properties of the leaflets in this study were restricted to non-physiologic magnitudes and the Reynolds number for blood flow was far below the magnitudes in the physiologic flow presumably due to numerical challenges. Kunzelman and colleagues performed FSI analyses of MV dynamics with the use of a neo-Hookean material for the MV leaflets and an assumption of a compressible fluid for the blood via an artificial compressibility approach.[29,55] The bulk modulus of blood was altered by several orders of magnitude for computational efficiency. Even though these FSI studies made significant advances in modeling the valve dynamics, the computational simulations were restricted to non-physiologic valve dynamics. Numerical difficulties in FSI analysis of complex valve dynamics must be overcome in order for such simulations to be applicable for a clinical setting.

In order to overcome the limitations on FSI analysis of tissue valve dynamics with physiologically realistic tissue material properties and flow Reynolds numbers, we are currently developing and testing an in-house FSI code. Our analysis methodology employs a partitioned approach for coupling the fluid and solid solvers.[19,90] Our flow solver employs a fixed Cartesian grid to avoid re-meshing of the rapidly deforming complex structure of the leaflets. Our structural solver, based on the open software (FEAP), employs experimentally derived nonlinear anisotropic material properties for the tissue valve leaflets[49,51,52] and published material property data for other valvular structures. This algorithm strongly couples the interface between the solid and the fluid using sub-iterations between partitioned solvers towards a robust and stable solutions for both solid and fluid. At the interface, an immersed interface-like approach[90,91] has been employed to incorporate the moving leaflets on the fluid as a source term in the momentum equation.

A high-order accurate time-splitting pressure correction scheme has been coupled with a FE solver in a strong fashion for FSI problems with added mass effects. The stability and convergence of the solver are enhanced by a combination of fictitious pressure and Aitken acceleration procedure. This high-fidelity moving boundary flow solver has been parallelized and scalable on state-of-the-art supercomputers. The solution fidelity is maintained using an adaptive octree meshing approach through a novel scalable mesh trimming procedure.[68]

Figure 5 demonstrates a prototype computational simulation of MV dynamics during diastole using our FSI algorithm. A patient MV model was obtained from 3D TEE data and placed in a simplified left ventricular chamber model with a flow inlet from the left atrium. Once diastole began, velocity increased at the inlet, pressure built up on the atrial side of the leaflet, the net force over the leaflets increased, and the MV began to open. Leaflet deformation was initiated near the annulus, marginal leaflet edge deformation followed, and the orifice expanded to fully open the leaflets. Negative velocity profiles were found in the axial flow contour indicating flow reversal behind both anterior and posterior leaflets during the opening phase. Structural analysis demonstrated larger stresses in the anterior leaflet compared to the posterior leaflet. With the specification of physiologically realistic material properties for the valvular apparatus and the blood, these computations will allow simulations of MV dynamics under physiologically realistic flow Reynolds numbers.

Future work

Great advancement in clinical imaging modalities and computational techniques over the last a few decades provides the promising potential to build a realistic 3D MV model and perform virtual simulations of MV function. It is anticipated that further improved computational techniques combined with the next generations of clinical imaging modalities will be developed for purely patient-specific, disease-specific, and case-specific computational MV evaluation and prediction of MVR through realistic virtual surgery simulations.

It is anticipated that fully validated and robust FSI algorithms will be available for MV dynamics analysis in the near future. Detailed FSI evaluation of normal MV function over the cardiac cycle will enable further understanding of the complex interaction between the MV apparatus components during MV function. Detailed structural dynamics of the MV leaflets and fluid dynamics in the LV chamber can be analyzed particularly in the filling and ejection phases of the cardiac cycle. Comparison of fluid dynamic alterations accompanied by the onset of MV diseases or following MVR will provide important information with respect to long-term effects on MV function. Such unified analyses are expected to be a valuable tool for comprehensive evaluation of MV dynamics aiding in early detection of the onset and stages of MV pathology and optimal pre-surgical planning of MVR.

Acknowledgements

This work was in part supported by the National Institutes of Health (R01 HL109597). The authors thank Drs. Vijay Govindarajan and John Mousel for providing supportive material and preliminary FSI simulation results of MV function.

References

1. Aarts PA, Steendijk P, Sixma JJ, Heethaar RM. Fluid shear as a possible mechanism for platelet diffusivity in flowing blood. J. Biomech. 1986; 19(10):799–805. [PubMed: 3782162]
2. Acar C, Farge A, Ramsheyi A, Chachques JC, Mihaileanu S, Gouezo R, Gerota J, Carpentier AF. Mitral valve replacement using a cryopreserved mitral homograft. Ann. Thorac. Surg. 1994; 57(3): 746–748. [PubMed: 8147653]
3. Ahmed S, Nanda NC, Miller AP, Nekkanti R, Yousif AM, Pacifico AD, Kirklin JK, McGiffin DC. Usefulness of transesophageal three-dimensional echocardiography in the identification of

individual segment/scallop prolapse of the mitral valve. Echocardiography. 2003; 20(2):203–209. [PubMed: 12848691]

4. Alfieri O, Maisano F, De Bonis M, Stefano PL, Torracca L, Oppizzi M, La Canna G. The double-orifice technique in mitral valve repair: a simple solution for complex problems. J. Thorac. Cardiovasc. Surg. 2001; 122(4):674–681. [PubMed: 11581597]
5. Argenziano M, Skipper E, Heimansohn D, Letsou GV, Woo YJ, Kron I, Alexander J, Cleveland J, Kong B, Davidson M, Vassiliades T, Krieger K, Sako E, Tibi P, Galloway A, Foster E, Feldman T, Glower D, Investigators E. Surgical revision after percutaneous mitral repair with the MitraClip device. Ann. Thorac. Surg. 2010; 89(1):72–80. discussion p 80. [PubMed: 20103209]
6. Avanzini A. A computational procedure for prediction of structural effects of edge-to-edge repair on mitral valve. J. Biomech. Eng. 2008; 130(3):031015. [PubMed: 18532864]
7. Barlow, JB.; Antunes, MJ. Functional anatomy of the mitral valve.. In: Barlow, JB., editor. Perspectives on the Mitral Valve. F. A. Davis Company; Philadelphia: 1987. p. 1-14.
8. Bhudia SK, McCarthy PM, Smedira NG, Lam BK, Rajeswaran J, Blackstone EH. Edge-to-edge (Alfieri) mitral repair: results in diverse clinical settings. Ann. Thorac. Surg. 2004; 77(5):1598–1606. [PubMed: 15111150]
9. Binder TM, Rosenhek R, Porenta G, Maurer G, Baumgartner H. Improved assessment of mitral valve stenosis by volumetric real-time three-dimensional echocardiography. J. Am. Coll. Cardiol. 2000; 36(4):1355–1361. [PubMed: 11028494]
10. Bortolotti U, Milano AD, Frater RW. Mitral valve repair with artificial chordae: a review of its history, technical details, long-term results, and pathology. Ann. Thorac. Surg. 2012; 93(2):684–691. [PubMed: 22153050]
11. Bothe W, Kuhl E, Kvitting JP, Rausch MK, Goktepe S, Swanson JC, Farahmandnia S, Ingels NB Jr. Miller DC. Rigid, complete annuloplasty rings increase anterior mitral leaflet strains in the normal beating ovine heart. Circulation. 2011; 124(11 Suppl):S81–96. [PubMed: 21911823]
12. Bothe W, Miller DC, Doenst T. Sizing for mitral annuloplasty: where does science stop and voodoo begin? Ann. Thorac. Surg. 2013; 95(4):1475–1483. [PubMed: 23481703]
13. Braunberger E, Deloche A, Berrebi A, Abdallah F, Celestin JA, Meimoun P, Chatellier G, Chauvaud S, Fabiani JN, Carpentier A. Very long-term results (more than 20 years) of valve repair with carpentier's techniques in nonrheumatic mitral valve insufficiency. Circulation. 2001; 104(12 Suppl 1):I8–11. [PubMed: 11568021]
14. Butany J, Collins MJ, David TE. Ruptured synthetic expanded polytetrafluoroethylene chordae tendinae. Cardiovasc. Pathol. 2004; 13(3):182–184. [PubMed: 15081477]
15. Carpentier, A.; Adams, DH.; Filsoufi, F. Carpentier's Reconstructive Valve Surgery. Elsevier Health Sciences; 2011. p. 368
16. Carpentier A, Relland J, Deloche A, Fabiani JN, D'Allaines C, Blondeau P, Piwnica A, Chauvaud S, Dubost C. Conservative management of the prolapsed mitral valve. Ann. Thorac. Surg. 1978; 26(4):294–302. [PubMed: 380485]
17. Chandran, KB.; Rittgers, SE.; Yoganathan, AP. Biofluid mechanics: the human circulation. CRC/Taylor & Francis; Boca Raton: 2007. p. 419
18. Chandran, KB.; Udaykumar, HS.; Reinhardt, J., editors. Image-based computational modeling of the circulatory and pulmonary systems. Springer Science+Business Media; New York: 2011. p. 465
19. Chandran KB, Vigmostad SC. Patient-specific bicuspid valve dynamics: overview of methods and challenges. J. Biomech. 2013; 46(2):208–216. [PubMed: 23182904]
20. Chang BC, Youn YN, Ha JW, Lim SH, Hong YS, Chung N. Long-term clinical results of mitral valvuloplasty using flexible and rigid rings: a prospective and randomized study. J. Thorac. Cardiovasc. Surg. 2007; 133(4):995–1003. [PubMed: 17382640]
21. Chaput M, Handschumacher MD, Tournoux F, Hua L, Guerrero JL, Vlahakes GJ, Levine RA. Mitral leaflet adaptation to ventricular remodeling: occurrence and adequacy in patients with functional mitral regurgitation. Circulation. 2008; 118(8):845–852. [PubMed: 18678770]
22. Choi A, Rim Y, Mun JS, Kim H. A novel finite element-based patient-specific mitral valve repair: virtual ring annuloplasty. Biomed. Mater. Eng. 2014; 24(1):341–347. [PubMed: 24211915]

23. Cohn LH, Couper GS, Aranki SF, Rizzo RJ, Kinchla NM, Collins JJ Jr. Long-term results of mitral valve reconstruction for regurgitation of the myxomatous mitral valve. J. Thorac. Cardiovasc. Surg. 1994; 107(1):143–150. discussion 150-141. [PubMed: 8283877]
24. Correale M, Ieva R, Di Biase M. Real-time three-dimensional echocardiography: an update. Eur. J. Intern. Med. 2008; 19(4):241–248. [PubMed: 18471671]
25. Dal Pan F, Donzella G, Fucci C, Schreiber M. Structural effects of an innovative surgical technique to repair heart valve defects. J. Biomech. 2005; 38(12):2460–2471. [PubMed: 16214494]
26. David TE, Ivanov J, Armstrong S, Rakowski H. Late outcomes of mitral valve repair for floppy valves: Implications for asymptomatic patients. J. Thorac. Cardiovasc. Surg. 2003; 125(5):1143–1152. [PubMed: 12771888]
27. David TE, Omran A, Armstrong S, Sun Z, Ivanov J. Long-term results of mitral valve repair for myxomatous disease with and without chordal replacement with expanded polytetrafluoroethylene sutures. J. Thorac. Cardiovasc. Surg. 1998; 115(6):1279–1285. discussion 1285-1276. [PubMed: 9628669]
28. De Hart J, Baaijens FP, Peters GW, Schreurs PJ. A computational fluid-structure interaction analysis of a fiber-reinforced stentless aortic valve. J. Biomech. 2003; 36(5):699–712. [PubMed: 12695000]
29. Einstein DR, Del Pin F, Jiao X, Kuprat AP, Carson JP, Kunzelman KS, Cochran RP, Guccione JM, Ratcliffe MB. Fluid-Structure Interactions of the Mitral Valve and Left Heart: Comprehensive Strategies, Past, Present and Future. International journal for numerical methods in engineering. 2010; 26(3-4):348–380. [PubMed: 20454531]
30. Ennis DB, Nguyen TC, Itoh A, Bothe W, Liang DH, Ingels NB, Miller DC. Reduced systolic torsion in chronic “pure” mitral regurgitation. Circ. Cardiovasc. Imaging. 2009; 2(2):85–92. [PubMed: 19808573]
31. Fedak PW, McCarthy PM, Bonow RO. Evolving concepts and technologies in mitral valve repair. Circulation. 2008; 117(7):963–974. [PubMed: 18285577]
32. Feldman T, Kar S, Rinaldi M, Fail P, Hermiller J, Smalling R, Whitlow PL, Gray W, Low R, Herrmann HC, Lim S, Foster E, Glower D, Investigators E. Percutaneous mitral repair with the MitraClip system: safety and midterm durability in the initial EVEREST (Endovascular Valve Edge-to-Edge REpair Study) cohort. J. Am. Coll. Cardiol. 2009; 54(8):686–694. [PubMed: 19679246]
33. Flachskampf FA, Chandra S, Gaddipatti A, Levine RA, Weyman AE, Ameling W, Hanrath P, Thomas JD. Analysis of shape and motion of the mitral annulus in subjects with and without cardiomyopathy by echocardiographic 3-dimensional reconstruction. J. Am. Soc. Echocardiogr. 2000:13277–287.
34. Gabbay U, Yosefy C. The underlying causes of chordae tendinae rupture: a systematic review. Int. J. Cardiol. 2010; 143(2):113–118. [PubMed: 20207434]
35. George KM, Mihaljevic T, Gillinov AM. Triangular resection for posterior mitral prolapse: rationale for a simpler repair. J. Heart Valve Dis. 2009; 18(1):119–121. [PubMed: 19301563]
36. Gillinov AM, Cosgrove DM. Minimally invasive mitral valve surgery: mini-sternotomy with extended transseptal approach. Semin. Thorac. Cardiovasc. Surg. 1999; 11(3):206–211. [PubMed: 10451251]
37. Gillinov AM, Cosgrove DM, Blackstone EH, Diaz R, Arnold JH, Lytle BW, Smedira NG, Sabik JF, McCarthy PM, Loop FD. Durability of mitral valve repair for degenerative disease. J. Thorac. Cardiovasc. Surg. 1998; 116(5):734–743. [PubMed: 9806380]
38. Glower DD. Surgical approaches to mitral regurgitation. J. Am. Coll. Cardiol. 2012; 60(15):1315–1322. [PubMed: 22939558]
39. Go AS, Mozaffarian D, Roger VL, Benjamin EJ, Berry JD, Blaha MJ, Dai S, Ford ES, Fox CS, Franco S, Fullerton HJ, Gillespie C, Hailpern SM, Heit JA, Howard VJ, Huffman MD, Judd SE, Kissela BM, Kittner SJ, Lackland DT, Lichtman JH, Lisabeth LD, Mackey RH, Magid DJ, Marcus GM, Marelli A, Matchar DB, McGuire DK, Mohler ER 3rd, Moy CS, Mussolino ME, Neumar RW, Nichol G, Pandey DK, Paynter NP, Reeves MJ, Sorlie PD, Stein J, Towfighi A, Turan TN, Virani SS, Wong ND, Woo D, Turner MB, C. American Heart Association Statistics, and S.

Stroke Statistics. Heart disease and stroke statistics--2014 update: a report from the American Heart Association. Circulation. 2014; 129(3):e28–e292. [PubMed: 24352519]

40. Hayek E, Gring CN, Griffin BP. Mitral valve prolapse. Lancet. 2005; 365(9458):507–518. [PubMed: 15705461]
41. Ho SY. Anatomy of the mitral valve. Heart. 2002; 88(Suppl 4):iv5–10. [PubMed: 12369589]
42. Hung J, Lang R, Flachskampf F, Shernan SK, McCulloch ML, Adams DB, Thomas J, Vannan M, Ryan T. 3D echocardiography: a review of the current status and future directions. J. Am. Soc. Echocardiogr. 2007; 20(3):213–233. [PubMed: 17336747]
43. Itoh A, Ennis DB, Bothe W, Swanson JC, Krishnamurthy G, Nguyen TC, Ingels NB Jr. Miller DC. Mitral annular hinge motion contribution to changes in mitral septal-lateral dimension and annular area. J. Thorac. Cardiovasc. Surg. 2009; 138(5):1090–1099. [PubMed: 19747697]
44. Jassar AS, Brinster CJ, Vergnat M, Robb JD, Eperjesi TJ, Pouch AM, Cheung AT, Weiss SJ, Acker MA, Gorman JH 3rd, Gorman RC, Jackson BM. Quantitative mitral valve modeling using real-time three-dimensional echocardiography: technique and repeatability. Ann. Thorac. Surg. 2011; 91(1):165–171. [PubMed: 21172507]
45. Kaji S, Nasu M, Yamamuro A, Tanabe K, Nagai K, Tani T, Tamita K, Shiratori K, Kinoshita M, Senda M, Okada Y, Morioka S. Annular geometry in patients with chronic ischemic mitral regurgitation: three-dimensional magnetic resonance imaging study. Circulation. 2005; 112(9 Suppl):I409–414. [PubMed: 16159855]
46. Kaplan SR, Bashein G, Sheehan FH, Legget ME, Munt B, Li XN, Sivarajan M, Bolson EL, Zeppa M, Arch MZ, Martin RW. Three-dimensional echocardiographic assessment of annular shape changes in the normal and regurgitant mitral valve. Am. Heart J. 2000; 139(3):378–387. [PubMed: 10689248]
47. Karlsson MO, Glasson JR, Bolger AF, Daughters GT, Komeda M, Foppiano LE, Miller DC, Ingels NB Jr. Mitral valve opening in the ovine heart. Am. J. Physiol. 1998; 274(2 Pt 2):H552–563. [PubMed: 9486259]
48. Kay GL, Aoki A, Zubiate P, Prejean CA Jr. Ruggio JM, Kay JH. Probability of valve repair for pure mitral regurgitation. J. Thorac. Cardiovasc. Surg. 1994; 108(5):871–879. [PubMed: 7967669]
49. Kim H, Chandran KB, Sacks MS, Lu J. An experimentally derived stress resultant shell model for heart valve dynamic simulations. Ann. Biomed. Eng. 2007; 35(1):30–44. [PubMed: 17089074]
50. Kim, H.; Lu, J.; Chandran, KB. Native human and bioprosthetic heart valve dynamics.. In: Chandran, KB.; Udaykumar, HS.; Reinhardt, J., editors. Image-based Computational Modeling of the Human Circulatory and Pulmonary Systems. Springer Science + Business Media; New York: 2011. p. 403-435.
51. Kim H, Lu J, Sacks MS, Chandran KB. Dynamic simulation pericardial bioprosthetic heart valve function. J. Biomech. Eng. 2006; 128(5):717–724. [PubMed: 16995758]
52. Kim H, Lu J, Sacks MS, Chandran KB. Dynamic simulation of bioprosthetic heart valves using a stress resultant shell model. Ann. Biomed. Eng. 2008; 36(2):262–275. [PubMed: 18046648]
53. Kunzelman K, Reimink MS, Verrier ED, Cochran RP. Replacement of mitral valve posterior chordae tendineae with expanded polytetrafluoroethylene suture: a finite element study. J. Card. Surg. 1996; 11(2):136–145. discussion 146. [PubMed: 8811408]
54. Kunzelman KS, Cochran RP, Chuong C, Ring WS, Verrier ED, Eberhart RD. Finite element analysis of the mitral valve. J. Heart Valve Dis. 1993; 2(3):326–340. [PubMed: 8269128]
55. Kunzelman KS, Einstein DR, Cochran RP. Fluid-structure interaction models of the mitral valve: function in normal and pathological states. Philos. Trans. R. Soc. Lond. B Biol. Sci. 2007; 362(1484):1393–1406. [PubMed: 17581809]
56. Kunzelman KS, Quick DW, Cochran RP. Altered collagen concentration in mitral valve leaflets: biochemical and finite element analysis. Ann. Thorac. Surg. 1998; 66(6 Suppl):S198–205. [PubMed: 9930448]
57. Kunzelman KS, Reimink MS, Cochran RP. Annular dilatation increases stress in the mitral valve and delays coaptation: a finite element computer model. Cardiovasc. Surg. 1997; 5(4):427–434. [PubMed: 9350801]

58. Kunzelman KS, Reimink MS, Cochran RP. Flexible versus rigid ring annuloplasty for mitral valve annular dilatation: a finite element model. J. Heart Valve Dis. 1998; 7(1):108–116. [PubMed: 9502148]
59. Lancellotti P, Moura L, Pierard LA, Agricola E, Popescu BA, Tribouilloy C, Hagendorff A, Monin JL, Badano L, Zamorano JL, E. European Association of. European Association of Echocardiography recommendations for the assessment of valvular regurgitation. Part 2: mitral and tricuspid regurgitation (native valve disease). Eur. J. Echocardiogr. 2010; 11(4):307–332. [PubMed: 20435783]
60. Lawrie GM. Mitral valve repair vs replacement. Current recommendations and long-term results. Cardiol. Clin. 1998; 16(3):437–448. [PubMed: 9742323]
61. Lawrie GM. Mitral valve: toward complete repairability. Surg. Technol. Int. 2006:15189–197.
62. Lawrie GM, Earle EA, Earle N. Intermediate-term results of a nonresectional dynamic repair technique in 662 patients with mitral valve prolapse and mitral regurgitation. J. Thorac. Cardiovasc. Surg. 2011; 141(2):368–376. [PubMed: 20416889]
63. Lim KH, Yeo JH, Duran CM. Three-dimensional asymmetrical modeling of the mitral valve: a finite element study with dynamic boundaries. J. Heart Valve Dis. 2005; 14(3):386–392. [PubMed: 15974534]
64. Maisano F, Redaelli A, Soncini M, Votta E, Arcobasso L, Alfieri O. An annular prosthesis for the treatment of functional mitral regurgitation: finite element model analysis of a dog bone-shaped ring prosthesis. Ann. Thorac. Surg. 2005; 79(4):1268–1275. [PubMed: 15797061]
65. Mansi T, Voigt I, Georgescu B, Zheng X, Mengue EA, Hackl M, Ionasec RI, Noack T, Seeburger J, Comaniciu D. An integrated framework for finite-element modeling of mitral valve biomechanics from medical images: application to MitralClip intervention planning. Med. Image Anal. 2012; 16(7):1330–1346. [PubMed: 22766456]
66. Marron K, Yacoub MH, Polak JM, Sheppard MN, Fagan D, Whitehead BF, de Leval MR, Anderson RH, Wharton J. Innervation of human atrioventricular and arterial valves. Circulation. 1996; 94(3):368–375. [PubMed: 8759078]
67. Mohty D, Orszulak TA, Schaff HV, Avierinos JF, Tajik JA, Enriquez-Sarano M. Very long-term survival and durability of mitral valve repair for mitral valve prolapse. Circulation. 2001; 104(12 Suppl 1):I1–I7. [PubMed: 11568020]
68. Mousel J, Govindarajan V, Udaykumar HS, Chandran KB. Investigation of physiologic flow-structure evolution in mechanical valve closure. World Congress of Biomechanics. 2014:W168.
69. Pouch AM, Xu C, Yushkevich PA, Jassar AS, Vergnat M, Gorman JH 3rd, Gorman RC, Sehgal CM, Jackson BM. Semi-automated mitral valve morphometry and computational stress analysis using 3D ultrasound. J. Biomech. 2012; 45(5):903–907. [PubMed: 22281408]
70. Pouch AM, Yushkevich PA, Jackson BM, Jassar AS, Vergnat M, Gorman JH, Gorman RC, Sehgal CM. Development of a semi-automated method for mitral valve modeling with medial axis representation using 3D ultrasound. Med. Phys. 2012; 39(2):933–950. [PubMed: 22320803]
71. Prot V, Haaverstad R, Skallerud B. Finite element analysis of the mitral apparatus: annulus shape effect and chordal force distribution. Biomechanics and modeling in mechanobiology. 2009; 8(1): 43–55. [PubMed: 18193309]
72. Rabbah JP, Saikrishnan N, Yoganathan AP. A novel left heart simulator for the multi-modality characterization of native mitral valve geometry and fluid mechanics. Ann. Biomed. Eng. 2013; 41(2):305–315. [PubMed: 22965640]
73. Reimink MS, Kunzelman KS, Cochran RP. The effect of chordal replacement suture length on function and stresses in repaired mitral valves: a finite element study. J. Heart Valve Dis. 1996; 5(4):365–375. [PubMed: 8858500]
74. Reimink MS, Kunzelman KS, Verrier ED, Cochran RP. The effect of anterior chordal replacement on mitral valve function and stresses. A finite element study. ASAIO J. 1995; 41(3):M754–762. [PubMed: 8573908]
75. Reul H, Talukder N, Muller EW. Fluid mechanics of the natural mitral valve. J. Biomech. 1981; 14(5):361–372. [PubMed: 7263728]
76. Rim Y, Laing ST, Kee P, McPherson DD, Kim H. Evaluation of mitral valve dynamics. JACC Cardiovasc. Imaging. 2013; 6(2):263–268. [PubMed: 23489540]

77. Rim Y, Laing ST, McPherson DD, Kim H. Mitral Valve Repair Using ePTFE Sutures for Ruptured Mitral Chordae Tendineae: A Computational Simulation Study. Ann. Biomed. Eng. 2014; 42(1): 139–148. [PubMed: 24072489]

78. Rim Y, McPherson DD, Chandran KB, Kim H. The effect of patient-specific annular motion on dynamic simulation of mitral valve function. J. Biomech. 2013; 46(6):1104–1112. [PubMed: 23433464]

79. Ryan LP, Jackson BM, Eperjesi TJ, Plappert TJ, St John-Sutton M, Gorman RC, Gorman JH 3rd. A methodology for assessing human mitral leaflet curvature using real-time 3-dimensional echocardiography. J. Thorac. Cardiovasc. Surg. 2008; 136(3):726–734. [PubMed: 18805278]

80. Sakamoto Y, Hashimoto K, Okuyama H, Ishii S, Hanai M, Inoue T, Shinohara G, Morita K, Kurosawa H. Long-term assessment of mitral valve reconstruction with resection of the leaflets: triangular and quadrangular resection. Ann. Thorac. Surg. 2005; 79(2):475–479. [PubMed: 15680818]

81. Salgo IS, Gorman JH 3rd, Gorman RC, Jackson BM, Bowen FW, Plappert T, St John Sutton MG, Edmunds LH Jr. Effect of annular shape on leaflet curvature in reducing mitral leaflet stress. Circulation. 2002; 106(6):711–717. [PubMed: 12163432]

82. Schwalm SA, Sugeng L, Raman J, Jeevanandum V, Lang RM. Assessment of mitral valve leaflet perforation as a result of infective endocarditis by 3-dimensional real-time echocardiography. J. Am. Soc. Echocardiogr. 2004; 17(8):919–922. [PubMed: 15282502]

83. Shi L, He Z. Hemodynamics of the mitral valve under edge-to-edge repair: an in vitro steady flow study. J. Biomech. Eng. 2009; 131(5):051010. [PubMed: 19388780]

84. Skallerud B, Prot V, Nordrum IS. Modeling active muscle contraction in mitral valve leaflets during systole: a first approach. Biomechanics and modeling in mechanobiology. 2011; 10(1):11–26. [PubMed: 20419330]

85. Spoor MT, Geltz A, Bolling SF. Flexible versus nonflexible mitral valve rings for congestive heart failure: differential durability of repair. Circulation. 2006; 114(1 Suppl):I67–71. [PubMed: 16820648]

86. Stevanella M, Maffessanti F, Conti CA, Votta E, Arnoldi A, Lombardi M, Parodi O, Caiani EG, Redaelli A. Mitral valve patient-specific finite element modeling from cardiac MRI: application to an annuloplasty procedure. Cardiovasc. Eng. Technol. 2011; 2(2):66–76.

87. Tamburino C, Ussia GP, Maisano F, Capodanno D, La Canna G, Scandura S, Colombo A, Giacomini A, Michev I, Mangiafico S, Cammalleri V, Barbanti M, Alfieri O. Percutaneous mitral valve repair with the MitraClip system: acute results from a real world setting. Eur. Heart J. 2010; 31(11):1382–1389. [PubMed: 20299349]

88. Timek TA, Miller DC. Experimental and clinical assessment of mitral annular area and dynamics: what are we actually measuring? Ann. Thorac. Surg. 2001; 72(3):966–974. [PubMed: 11565706]

89. Verhey JF, Nathan NS, Rienhoff O, Kikinis R, Rakebrandt F, D'Ambra MN. Finite-element-method (FEM) model generation of time-resolved 3D echocardiographic geometry data for mitral-valve volumetry. Biomed Eng Online. 2006:517.

90. Vigmostad S, Udaykumar HS, Lu J, Chandran KB. Fluid-structure interaction methods in biological flows with specific emphasis on heart valve dynamics. Int J Numerical Methods in Biomed Eng. 2010:26435–470.

91. Vigmostad, SC.; Udaykumar, HS. Algorithms for fluid-structure interaction.. In: Chandran, KB.; Udaykumar, HS.; Reinhardt, J., editors. Image-based computational modeling of the human circulatory and pulmonary systems. Springer Science+Business Media; New York: 2011. p. 191-234.

92. Votta E, Caiani E, Veronesi F, Soncini M, Montevecchi FM, Redaelli A. Mitral valve finite-element modelling from ultrasound data: a pilot study for a new approach to understand mitral function and clinical scenarios. Philosophical transactions. Series A, Mathematical, physical, and engineering sciences. 2008; 366(1879):3411–3434.

93. Votta E, Le TB, Stevanella M, Fusini L, Caiani EG, Redaelli A, Sotiropoulos F. Toward patient-specific simulations of cardiac valves: state-of-the-art and future directions. J. Biomech. 2013; 46(2):217–228. [PubMed: 23174421]

94. Votta E, Maisano F, Bolling SF, Alfieri O, Montevecchi FM, Redaelli A. The Geoform disease-specific annuloplasty system: a finite element study. Ann. Thorac. Surg. 2007; 84(1):92–101. [PubMed: 17588392]

95. Votta E, Maisano F, Soncini M, Redaelli A, Montevecchi FM, Alfieri O. 3-D computational analysis of the stress distribution on the leaflets after edge-to-edge repair of mitral regurgitation. J. Heart Valve Dis. 2002; 11(6):810–822. [PubMed: 12479282]

96. Wang Q, Sun W. Finite element modeling of mitral valve dynamic deformation using patient-specific multi-slices computed tomography scans. Ann. Biomed. Eng. 2013; 41(1):142–153. [PubMed: 22805982]

97. [Accessed 26 Mar 2014] Cleveland Clinic. [www.clevelandclinicmeded.com/medicalpubs/diseasemanagement/cardiology/mitral-valve-disease/]

98. Wong VM, Wenk JF, Zhang Z, Cheng G, Acevedo-Bolton G, Burger M, Saloner DA, Wallace AW, Guccione JM, Ratcliffe MB, Ge L. The effect of mitral annuloplasty shape in ischemic mitral regurgitation: a finite element simulation. Ann. Thorac. Surg. 2012; 93(3):776–782. [PubMed: 22245588]

99. Xie MX, Wang XF, Cheng TO, Wang J, Lu Q. Comparison of accuracy of mitral valve area in mitral stenosis by real-time, three-dimensional echocardiography versus two-dimensional echocardiography versus Doppler pressure half-time. Am. J. Cardiol. 2005; 95(12):1496–1499. [PubMed: 15950582]

100. Xu C, Jassar AS, Nathan DP, Eperjesi TJ, Brinster CJ, Levack MM, Vergnat M, Gorman RC, Gorman JH 3rd, Jackson BM. Augmented mitral valve leaflet area decreases leaflet stress: a finite element simulation. Ann. Thorac. Surg. 2012; 93(4):1141–1145. [PubMed: 22397985]

101. Zamorano J, Cordeiro P, Sugeng L, Perez de Isla L, Weinert L, Macaya C, Rodriguez E, Lang RM. Real-time three-dimensional echocardiography for rheumatic mitral valve stenosis evaluation: an accurate and novel approach. J. Am. Coll. Cardiol. 2004; 43(11):2091–2096. [PubMed: 15172418]

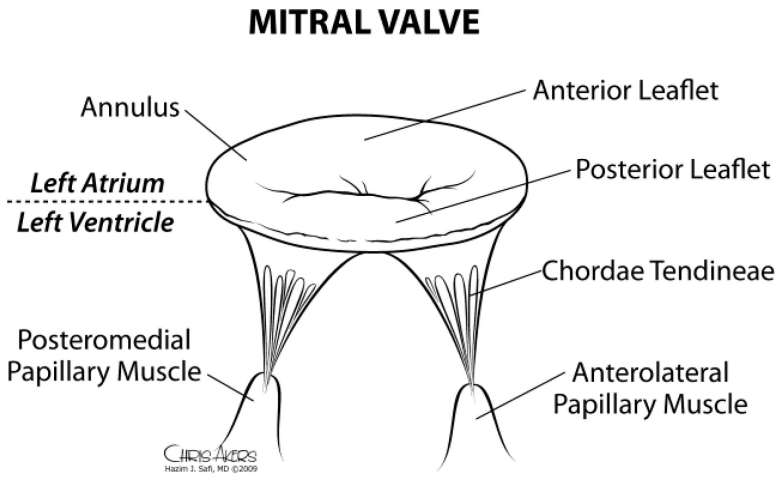

Figure 1.
Schematic of the MV apparatus.

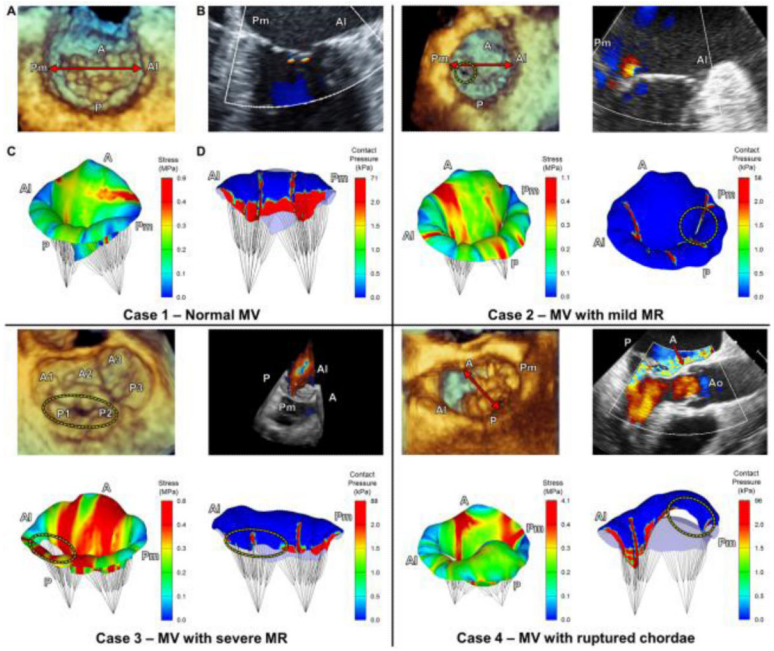

Figure 2.

Representative clinical case studies of patient-specific computational MV evaluation: normal, mild MR, severe MR, and ruptured chordae. (A) Volumetric MV image from 3D TEE data, (B) Doppler TEE image, (C) Leaflet stress distribution, (D) Leaflet contact distribution (redrawn with modification from Rim et al.[76]). A – anterior; P – posterior; Al – anterolateral; Pm – posteromedial; Ao – Aorta.

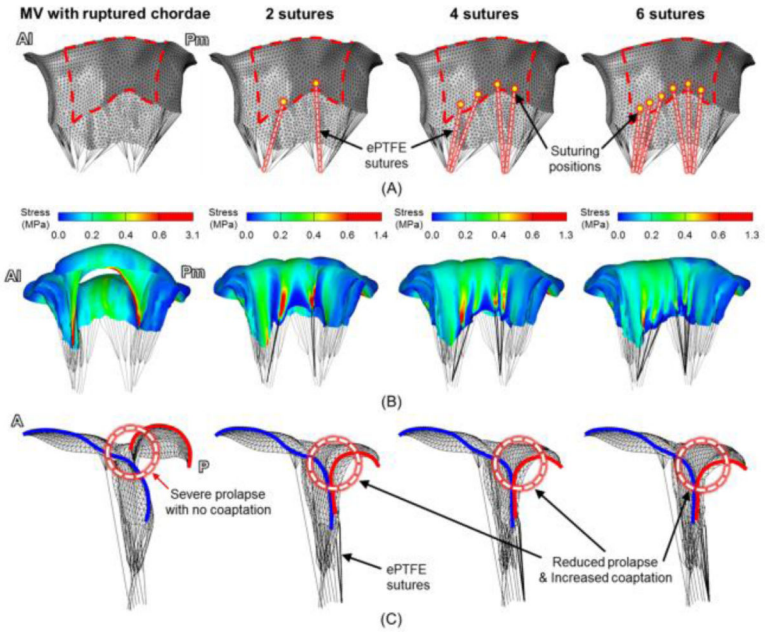

Figure 3.

Patient-specific virtual chordal replacement simulations. (A) Simulation protocol for virtual chordal replacement using two, four and six ePTFE sutures, (B) Stress distributions across the MV leaflets and annulus before and after virtual chordal replacement, (C) Leaflet morphologies before and after virtual chordal replacement (redrawn with modification from Rim et al.[77]).

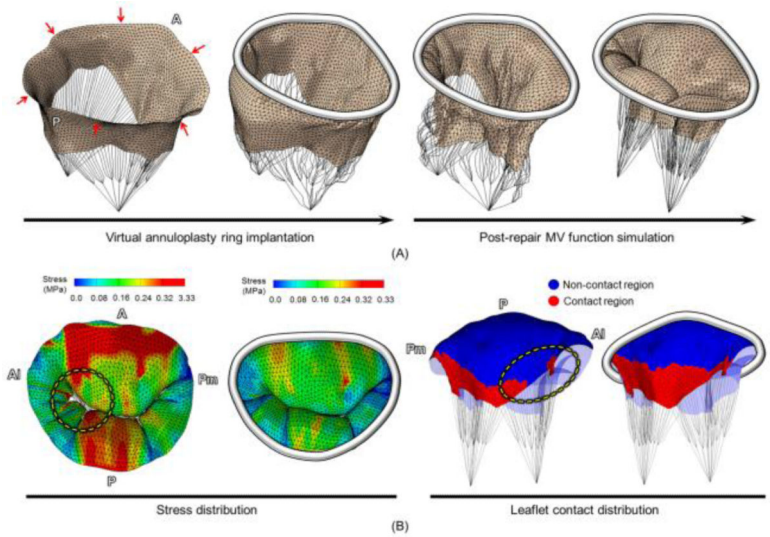

Figure 4.

Patient-specific virtual ring annuloplasty simulation. (A) Virtual ring annuloplasty protocol, (B) Stress and leaflet contact distributions across the MV leaflets before and after virtual ring annuloplasty (redrawn with modification from Choi et al.[22]).

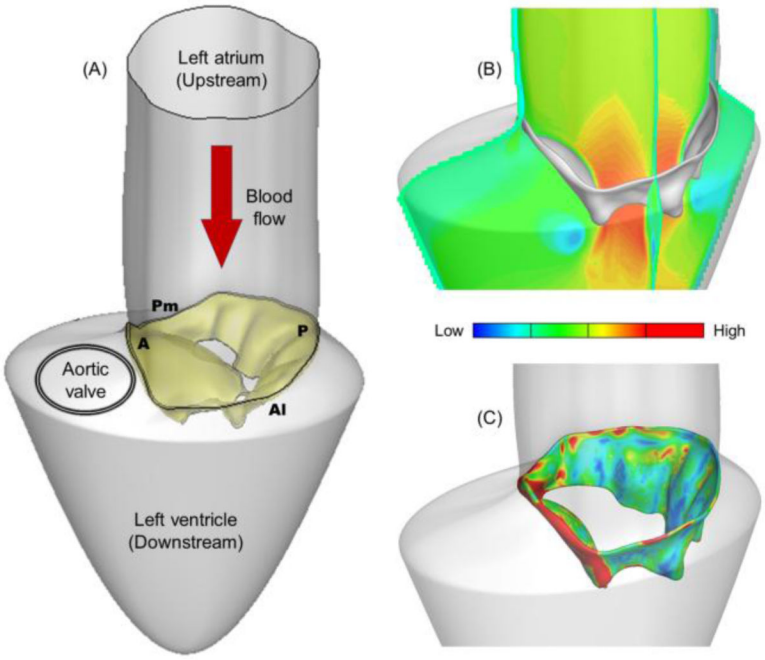

Figure 5.

A prototype FSI simulation of MV dynamics. (A) A patient MV model from 3D TEE data placed in a simplified left ventricular chamber model, (B) Axial velocity profiles of the blood flow across the MV during diastole, (C) Stress distribution over the MV leaflets.